[2]J. G. Dash and M. Bretz, Phys. Rev. 174, 247 (1968); H. W. Jackson, *ibid.* 180, 184 (1969); F. Ricca, C. Pisani, and E. Garrone, J. Chem. Phys. 51, 4079 (1969); A. Novaco and F. J. Milford (unpublished); H-W. Lai, C-W. Woo, and F. Y. Wu (unpublished).

[3]M. Schick and C. E. Campbell, Phys. Rev. A 2, 1591 (1970).

[4]D. S. Hyman, Report No. 1273, Material Science Center, Cornell University, Ithaca, N. Y. (unpublished).

[5]J. de Boer and A. Michels, Physica 5, 945 (1938).

[6]F. London, *Superfluids* (Wiley, New York, 1954), Vol. II.

[7]M. Schick, Phys. Rev. A (to be published).

[8]W. H. Keesom and K. W. Taconis, Physica 5, 270 (1938).

[9]This conclusion, which is applicable at the absolute zero of temperature and to a large but finite system of particles, is not directly related to the observation that an infinite two-dimensional solid is unstable at any finite temperature. This latter observation has been proved by N. D. Mermin, Phys. Rev. 176, 250 (1968).

[10]W. L. McMillan, Phys. Rev. 138, A442 (1965).

[11]D. Schiff and L. Verlet, Phys. Rev. 160, 208 (1967).

[12]W. Massey and C. W. Woo, Phys. Rev. 164, 207 (1967).

[13]A. Bijl, Physica 7, 869 (1940); N. F. Mott, Phil. Mag. 40, 61 (1949); R. B. Dingle, *ibid.* 40, 573 (1949); R. Jastrow, Phys. Rev. 98, 1479 (1955).

[14]A. Rahman, Phys. Rev. 136, A405 (1964).

[15]A. Rahman (private communication).

[16]H. W. Jackson and E. Feenberg, Ann. Phys. (N.Y.) 15, 266 (1961).

[17]C. E. Campbell and E. Feenberg, Phys. Rev. 188, 396 (1969).

[18]T. B. Davison and E. Feenberg, Ann. Phys. (N.Y.) 53, 559 (1969).

PHYSICAL REVIEW A VOLUME 3, NUMBER 2 FEBRUARY 1971

Heat Capacity near the Superfluid Transition in He^4 at Saturated Vapor Pressure

Guenter Ahlers
Bell Telephone Laboratories, Murray Hill, New Jersey 07974
(Received 24 June 1970)

Apparatus and experimental procedures suitable for a number of high-precision measurements of properties of liquid helium near the superfluid transition temperature T_λ are described. Experimental determinations near T_λ of the heat capacity at saturated vapor pressure are presented. On the basis of these measurements, the asymptotic temperature dependence of the heat capacity at constant pressure C_p is examined and compared with current theories of critical phenomena. Although there is some latitude in the interpretation of the results in terms of the asymptotic behavior of C_p, no interpretation fully in agreement with the original formulations of the scaling laws for critical phenomena, and with a divergent C_p, is consistent with the measurements. It is expected that an extensive discussion of the thermodynamics of the λ line at higher pressure, based on measurements of the heat capacity at constant volume C_v, will be presented in a later publication.

I. INTRODUCTION

In recent years it has been possible to measure rather accurately a number of equilibrium[1-13] and transport[14-20] properties near the superfluid transition temperature T_λ in He^4. Some of these measurements have been used[7,14-16,21] to verify rather accurately predictions based upon the so-called scaling laws[22-27] which relate the temperature dependences of various parameters near critical points. There exist already very detailed measurements of the heat capacity at saturated vapor pressure[1-5] C_s for He^4 near T_λ. However, developments in low-temperature techniques and instrumentation which have occurred since the time of this work make it possible to improve considerably upon these earlier results, and to establish the detailed nature of the divergence of the heat capacity at constant pressure C_p more precisely. It seems particularly desirable to study the divergence of C_p in great detail for the superfluid transition. This system is extremely suitable for high-precision experimental work, and one can hope to put theoretical predictions[22-27] to a more severe test here than is possible near most other critical points. Some of the well-known advantages from an experimental viewpoint of the superfluid transition are the relative ease of attaining thermal equilibrium, even for He I, the high purity of the sample, and the ease with which corrections for the gravitational pressure gradient[28] in the sample can be applied. We therefore have attempted to measure C_s as precisely as can reasonably be done at this time. These new results are in very good agreement with the earlier work.[1-5] Extremely near the transition, where the precision of the measurements is limited by the temperature resolution, the new data are only about a factor of 2 more precise than the older ones. Further away from T_λ, where the precision is limited by other calorimetric techniques, the new results constitute

an improvement over the older ones by about an order of magnitude. Because of this greater precision, an asymmetry in C_p near the transition was revealed which had not been observed previously, and which is contrary to the original scaling-law formulation[22-24] if C_p diverges. This observation will require some modification in the theory if a divergent C_p is to be retained, and if exact agreement between scaling predictions and experimental measurements are desired. An attempt at modifying the original formulation of scaling and to achieve consistency between theory and experiment already has been made by Fisher.[29]

The main features of the results of the work presented in this paper have been reported briefly elsewhere.[28,30,31]

The remainder of this paper is divided into several sections. In Sec. II, the experimental aspects of this work are described. This is done in four subsections, with one each devoted to the apparatus, to various calibrations, to the experimental procedure, and to the performance of various parts of the apparatus during measurements. Considerable detail is given because the same apparatus has been used to obtain a number of previously published results,[14,15,32,33] because it will be used for further measurements on liquid helium under pressure, and because it has not been described elsewhere. Section III is devoted to data analysis. Here various corrections to the primary measurements are discussed, and probable systematic and random errors are estimated. In addition, the functional form in terms of which C_p is to be interpreted is discussed and the least-squares procedure used for the data analysis is described. In Sec. IV, pertinent theoretical predictions based upon scaling-law theory are reviewed briefly. In Sec. V, the measurements at saturated vapor pressure are presented and discussed. In Sec. VI, the conclusions to be derived from this work are summarized.

We have omitted in this paper a discussion of various interesting aspects of the thermodynamics of λ lines, although the experimental results have a strong bearing upon these problems. Much of the basis for a thorough thermodynamic analysis of λ lines already has been presented elsewhere.[34] However, a complete treatment of this problem requires a knowledge of the pressure derivatives of C_p, and experimental measurements under pressure which will yield these derivatives are still being pursued. After the completion of that work we expect to present a complete discussion of the thermodynamics of the transition, and to extend the comparison with scaling to higher pressures. A brief indication of the consistency of some of the measurements under pressure and the results obtained at saturated vapor pressure has been given previously.[30]

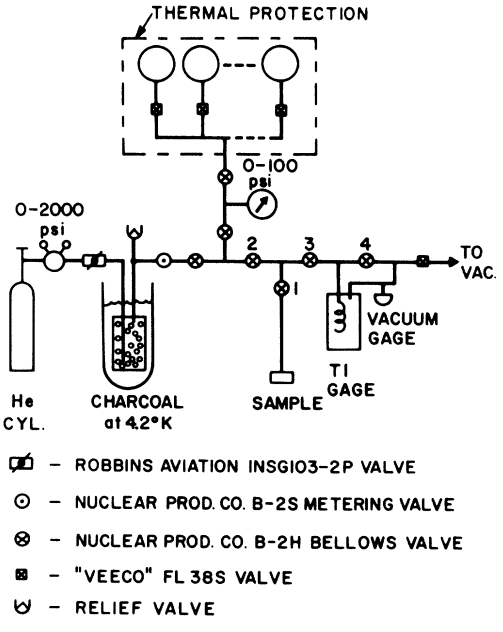

FIG. 1. Schematic diagram of the sample preparation system.

II. EXPERIMENTAL

A. Apparatus

1. *Gas Preparation and Measuring System*

A schematic diagram of the system is shown in Fig. 1. The helium sample originated in a commercial cylinder, was purified at 4.2 °K, and could be admitted through a needle valve to a sample manifold. Attached to this manifold were the sample cell, a gas-volume measuring system, a Texas Instruments quartz-bourdon-tube (TI) gauge, and a vacuum system. The sample cell will be described in Sec. II A 2, and details about the TI gauge will be given in Sec. II B 2.

The gas-volume measuring system consisted of nine separate volumes, connected to each other by their own manifold, ranging in size from 1 to 20 liter, and having a total volume of nominally 75 liter. It was contained in a large copper and Styrofoam lined box which provided protection from room-temperature variations. The stability of the temperature inside the box was of the order of 0.1 °C/h.

The sample manifold contained Nuclear Products Co. type B-2H bellows valves, and all volumes were minimized wherever important. The TI bourdon tube was connected to the sample manifold by means of about 40 cm of 0.03-cm-i.d. tubing. A pressure equilibration valve (not shown in Fig. 1) was installed between the bourdon tube and the reference vacuum directly at the TI gauge to permit the de-

termination of the gauge reading at zero differential pressure.

2. *Calorimeter and Sample Cell*

A schematic diagram of the calorimeter is shown in Fig. 2. This assembly was immersed in a liquid-helium bath which could be cooled to 1.3 °K. The liquid-helium sample was contained in a copper cell which was connected to the external sample manifold (see Fig. 1) by means of a stainless-steel capillary (0.02-cm-i.d. ×0.01-cm wall), and which was suspended from cotton strings in the main vacuum. The sample cell was 1.59 cm high and had a diameter of 8.3 cm. It was partially occupied by a mesh of fine copper wires. Attached to the bottom of the sample cell was a second, much smaller cell (to be referred to as the probe) which was 0.95 cm high and had a diameter of 0.93 cm.[35] The probe was internally connected to the sample cell by a hole of 0.04-cm diam and 1.59-cm length. It had 0.015-cm-thick stainless-steel walls, was sealed to the sample cell by an indium gasket, and had a copper bottom to which it was sealed by a second indium gasket. The purpose of the probe was to determine the transition temperature by measuring the onset of resistance to heat flow. The capillary passed through the main vacuum for a length of 8 cm, and then entered a separate vacuum system. This capillary vacuum consisted of a stainless-steel tube of 0.95-cm diam and 0.025-cm-thick walls, and protruded into the main vacuum chamber by about 6 cm. A copper wire provided a thermal connection between the helium bath (1.3 °K) and the bottom of the capillary vacuum with about 10^{-3} W/°K conduction. The temperature could be regulated at the bottom of the capillary vacuum by means of a heater, a thermometer, and a simple electronic circuit with a precision of $\pm 10^{-4}$ °K.[36] Inside the capillary vacuum, and attached to the capillary, were another heater and thermometer which could be used to assure that the temperature along the capillary was higher everywhere than the sample temperature. This is necessary to avoid condensation of liquid in the capillary during measurements of C_s.

In order to provide maximum thermal stability for the sample, all electrical leads and the cotton strings from which the sample was suspended were thermally attached to an isothermal platform, and then brought down to the sample. The platform was connected to the bath by a heat leak of about 10^{-5} W/°K. By means of a heater, a thermometer, and another regulator circuit its temperature could be held constant to $\pm 10^{-5}$ °K. The platform was usually maintained at about 1.6 °K. This arrangement provided adequate thermal stability for the sample, and its was found unnecessary to regulate the temperature of the main helium bath.

Since it was necessary to dissipate power at the sample cell during measurements ($\approx 10^{-6}$ W), the sample, by virtue of its good thermal isolation, normally would have warmed slowly. Therefore, a small heat leak ($\approx 2\times 10^{-6}$ W/°K) was introduced between the sample cell and the isothermal platform. Attached to the bottom of this thermal connection was an auxiliary heater which could be used to counteract the heat leak when desired. With this arrangement one can estimate that conduction-heat transfer exclusive of the capillary was stable to about 10^{-10} W, and did not limit the thermal stability of the system. Room-temperature radiation-heat inputs were rendered negligible by covering the main vacuum-pump line with a cap which was thermally attached to the bath.

Attached to the sample cell were a heater and a thermometer which will be referred to as the main heater and the main thermometer. In addition, there were two other thermometers, one on the sample cell, and one at the bottom of the probe. The latter two thermometers were operated as two arms of an ac bridge, and measured the temperature difference between the top and bottom of the probe. Jointly, they will be referred to as the differential thermometer. The thermometer circuits have been described in detail elsewhere.[28]

The main heater consisted of 5682 Ω of 0.0038-cm-diam double polyurethane-insulated Karma wire (Driver-Harris Co.). It was provided with two current and two potential leads. The current leads between the isothermal platform and the sample cell had a resistance of about 10 Ω each, and half of

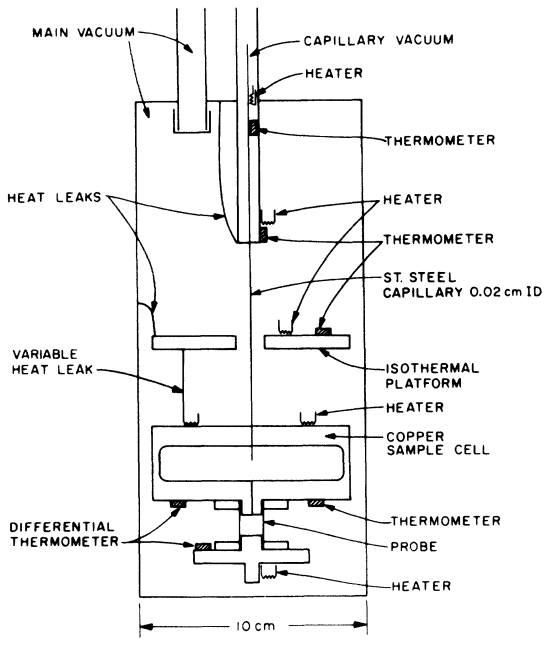

FIG. 2. Schematic diagram of the calorimeter.

their total resistance was included in the heater resistance for calculating the heater power.

Each of the three thermometers on the sample cell and probe consisted of 20 "ohmite" (Allen Bradley), nominally 56 Ω, $\frac{1}{8}$ W, carbon composition resistors connected in series. The resistors were ground flat on one side, and glued with GE 7031 varnish side by side onto a copper plate covered with 6×10^{-4}-cm-thick Mylar. The entire bank of resistors was then ground flat on the exposed side, and glued to a second copper plate, again with Mylar for electrical insulation. The two copper plates were thermally attached at the desired point of the system. The purpose of this arrangement was to provide good thermal contact between the thermometers and the point at which the temperature was to be measured, so as to allow reasonably large power dissipation in the thermometers without excessive self-heating.

Finally, it should be mentioned that there was yet another heater of about 5-kΩ resistance at the bottom of the probe. However, this heater was used only in conjunction with measurements other than those to be discussed here.[14,15]

All electrical leads required inside the main vacuum were brought into the system through the main vacuum-pump line. Down to the bottom of this pump line they consisted of quadrupule Formvar-insulated 7.5×10^{-3}-cm-diam copper wires. Upon entering the main vacuum, they were thermally attached to the bath, and converted to quadruple Formvar-insulated 7.5×10^{-3}-cm-diam manganin wires. The manganin wires were again thermally attached to the bath, and then to the isothermal platform. Those leads which were required at the sample were thermally attached to the sample cell before being brought to the desired heater or thermometer. In addition, the leads needed at the bottom of the probe were thermally attached there before being connected to the thermometer. The leads to be used for the main thermometer were physically kept apart from those to be used for the differential thermometer to minimize interference between the two systems. Wherever good electrical isolation from ground was necessary, thermal attachment of leads was made only through 6×10^{-4}-cm-thick Mylar.

TABLE I. System volumes in cm^3.

Sample cell exclusive of capillary, 2 °K	81.53
Sample cell and capillary up to valve[a] 1, R. T.	82.5 ±0.4
Between valves[a] 1, 2, and 3	0.83
Between valves[a] 3 and 4	2.56
Capillary up to valve[a] 1 (calculated)	0.07

[a]Valve numbers refer to Fig. 1.

B. Calibrations

1. *Volumes*

Volumes at room temperature were calibrated by measuring the change in pressure associated with the expansion of helium gas from reference vessels into unknown volumes. The reference volumes were calibrated with an accuracy of 0.01% by weighing the vessels empty and when filled with distilled water. Volumes in the Stryofoam-insulated box were determined with an accuracy of 0.1%, and the much smaller volumes in the vicinity of the sample manifold were calibrated with an accuracy of about 1%. A few volumes which are particularly important for corrections to the measurements are listed in Table I.

In order to determine the cell volume at low temperature, the cell was filled almost completely with liquid helium at 2.17 °K. The temperature of the cell was then reduced. The consequent expansion of the liquid (liquid helium has a negative thermal-expansion coefficient in this temperature range) caused the cell to be overfilled at 2 °K. Then the cell was heated slowly, and the sample pressure was monitored. The pressure decreased until the liquid level left the capillary, and then followed the vapor-pressure curve. From this, it was deduced that the cell was filled completely at 2.14 °K. The sample was then expanded into the gas-volume measuring system, and the entire apparatus was warmed to room temperature. It was deduced that the cell had contained 2.974 moles. A molar volume of 27.413 cm^3 for liquid helium at saturated vapor pressure and 2.14 °K[37] yielded a cell volume (including the probe) of 81.53 cm^3. It is estimated that the sample mass is known with an accuracy of 0.2%.

2. *Pressure Gauge*

Pressures were measured with a Texas Instruments model No. 145 precision pressure gauge (serial No. 1344) with micron gearing containing a Texas Instruments quartz-bourdon tube type 1 (serial No. 2564) with a range from 0 to 2580 Torr. The sensitivity of the gage was nominally 0.0082 Torr/minor division. Using the instrument in the external mode, a pressure resolution of 0.002 Torr ($\frac{1}{4}$ minor division) was possible.

The pressure gauge had been calibrated by the manufacturer on 11-11-67 at 20 points. The calibration pressure P and the ratio G between the pressure and the gauge reading at these 20 points were fitted to the relation

$$P_c = A_1 G + B_1 G^2 \tag{1}$$

by a least-squares procedure. The calculated pressures P_c were then subtracted from the calibration pressures P. The differences $\Delta P = P - P_c$ are

shown in Fig. 3 as open circles.

The lowest pressure at which a calibration point had been furnished by the manufacturer was 129 Torr. Since this is higher than the pressure range of interest for vapor-pressure thermometry, the gauge was also calibrated (on 11-22-68) against a mercury manometer between 54 and 800 Torr with an accuracy of 0.05 Torr and, for pressures less than 54 Torr, against an oil manometer with an accuracy of 0.1% of P and a precision of 6×10^{-3} Torr. The original parameters in Eq. (1) were retained; but additional points on the difference graph were computed from these data, and are shown in Fig. 3 as solid circles. The largest difference between the manufacturer's calibration and the one carried out here is 0.2 Torr at 800 Torr, or 0.025%.

For the low-pressure range of the oil manometer, ΔP is shown as a function of P on an expanded scale in Fig. 4. It is seen that ΔP can be represented by an oscillatory function of P with an amplitude of about 0.04 Torr, or 5 minor gauge divisions, and a periodicity of about 25 Torr, or 3000 minor gauge divisions. Pressures were computed from gauge readings using Eq. (1) in conjunction with the difference graphs shown in Figs. 3 and 4. For pressures below 60 Torr, the oscillatory behavior of the difference graph was considered. At higher pressures, where this oscillatory behavior is not known experimentally because of the lower resolution of the mercury manometer, a smooth nonoscillatory curve through the calibration points was used. If the oscillatory component is independent of pressure, then errors due to the procedure adopted above 60 Torr do not exceed 0.04 Torr for the pressure and 1% for pressure derivatives.

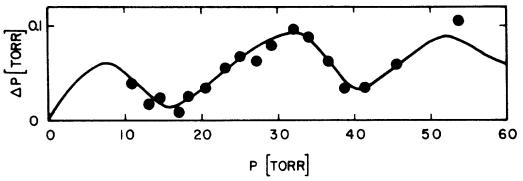

FIG. 4. Deviations at small pressures of calibration points from this work for the Texas Instruments bourdon-tube pressure gauge from Eq. (1).

3. *Main Thermometer*

The bridge ratio R for the main thermometer was calibrated against the vapor pressure of He^4 on the 1958 He^4 scale of temperatures (T_{58}).[38] For this purpose, the sample vapor pressure was measured with the gauge described above. The measurements had a resolution of 2×10^{-5} °K near 2 °K, corresponding to 2×10^{-3} Torr. Systematic errors due to the pressure-gauge calibration do not exceed 0.1% of the vapor pressure, or 5×10^{-4} °K near T_λ. Since the vapor pressure of the sample was measured through a capillary tube, a small mildly temperature-dependent correction had to be applied for the thermomolecular pressure ratio.[39]

The thermometer was recalibrated whenever it had been cooled from room temperature. In order to demonstrate the effect of thermal cycling upon the thermometer calibration, the data obtained during one thermal cycle (8-7-68) were fitted to the equation[40]

$$T_c = (\log_{10}R)/[A + B\log_{10}R + C(\log_{10}R)^2] \qquad (2)$$

by a least-squares procedure. The deviations $\Delta = T - T_c$ from this equation of data obtained for three separate calibrations are shown in Fig. 5.

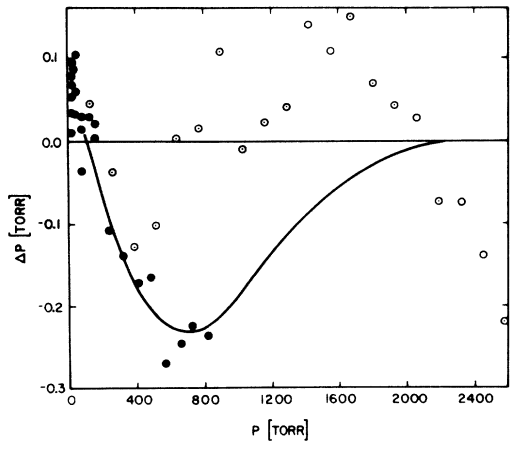

FIG. 3. Deviations of calibration points for the Texas Instruments bourdon-tube pressure gauge from Eq. (1). Open points represent the manufacturer's calibration, and solid points are from this work.

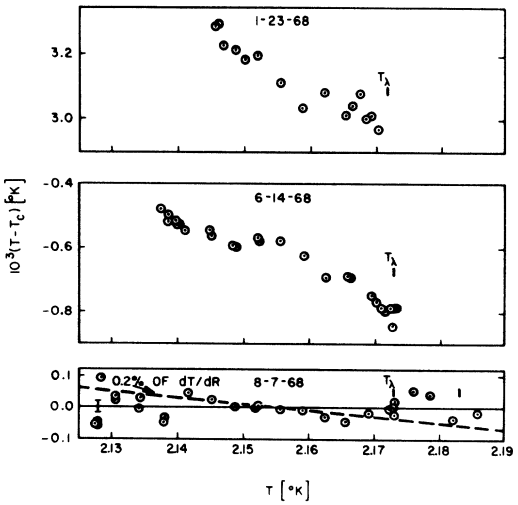

FIG. 5. Deviations of the thermometer calibration from Eq. (2).

It is apparent that the temperature resolution based on the expected pressure resolution of about 2×10^{-5} °K is only slightly smaller than the scatter in Δ. From the calibration of 8-7-68, it can be seen that Eq. (2) represents the data well, and that deviations from this equation are not systematic. The standard error for these data is 4×10^{-5} °K. Comparison of the three calibrations reveals that both Δ and $d\Delta/dT$ changed slightly upon thermal cycling.

In addition to the change of the thermometer calibration upon thermal cycling, it was observed also that the thermometer bridge ratio R_λ at T_λ was time dependent. On one occasion, the derivative dR_λ/dt (t is the time) was measured repeatedly over a 50-day period without warming the thermometer above 2.2 °K. The results of these measurements are shown in Fig. 6. It is apparent that the thermometer initially after cooling from room temperature undergoes measurable changes, and stabilizes only after many days have elapsed. Nonetheless, after a few days the resistance change with time corresponds only to an apparent change of the temperature of 10^{-4} °K/day. The magnitude of dR_λ/dt observed here is the same as that observed previously for a similar carbon thermometer in a rather different experimental arrangement[28] and probably can be regarded as typical for a thermometer of this type which has been aged at low temperature for several days.

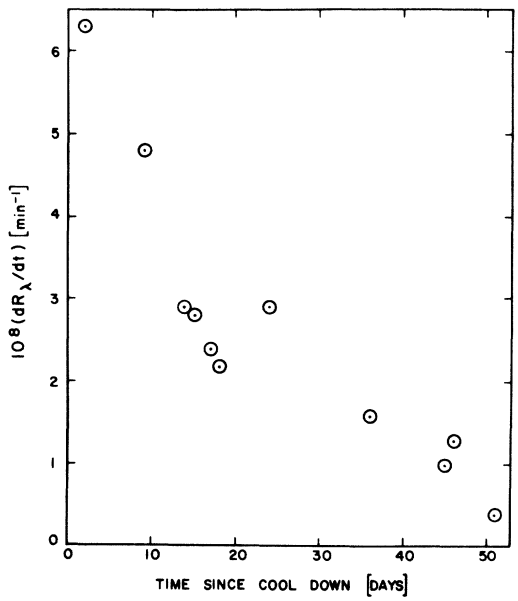

FIG. 6. Drift rate of the thermometer bridge ratio as a function of the time elapsed since the apparatus was cooled below 2.2 °K. 1×10^{-8} min^{-1} for dR_λ/dt corresponds to an apparent temperature change of 3×10^{-8} °K/min.

C. Procedure

The system was cooled to 20.3 °K by using hydrogen exchange gas in the main vacuum system, and by transferring first liquid nitrogen and then liquid hydrogen into the Dewar. This required about 7 h. During this procedure, a sample pressure of about 1 bar was maintained, and helium exchange gas was kept in the capillary vacuum. The hydrogen exchange gas was then removed, and liquid helium substituted for the liquid hydrogen in the Dewar. From about 20 °K to the lowest temperature, cooling of the cell was caused only by admission of the cold sample and by heat carried by superfluid in the capillary. In order to achieve this cooling, the bath was pumped to 1.3 °K. Helium gas was then supplied to the capillary from the sample manifold at an external pressure of about 3 bars. After approximately 1 h, the cell had cooled to about 3 °K by virtue of the cold gas entering through the capillary. At this point, the cell was still only partially occupied by liquid. Cooling to the lowest temperature ($\approx$1.7 °K) was then accomplished in an additional 4 h by the superfluid film flow in the capillary. After the cell was well below T_λ, it was slightly overfilled with liquid by admitting more gas in the capillary. It was possible to tell when the cell was full both from a record of the cell temperature and from the pressure in the sample manifold. The exchange gas in the capillary vacuum was then removed. Next, with the cell at about 2.17 °K, a small amount of sample was pumped out of the cell when it was desired to measure the heat capacity at saturated vapor pressure. As the liquid level dropped in the capillary, the helium pressure gradually dropped to the sample vapor pressure. Thereafter, removal of more sample became extremely slow because of the small pressure drop across the capillary. After pumping on the sample overnight, the cell at 2.17 °K was still almost filled, and was found to be completely filled at 2.14 °K (see Sec. II B 1). It is evident that a sample prepared in this manner has an extremely small vapor volume. During the measurements of C_s, valve 1 (Fig. 1) was kept closed so as to minimize the system volume not occupied by liquid.

Whenever there was liquid in the sample cell, control of the temperature at the bottom of the capillary vacuum (to be referred to as T') provided a convenient "heat switch." When T' was less than the sample temperature T and also less than T_λ, the sample cooled at an appreciable rate either because of He II film flow or because of heat transfer in bulk He II in the capillary. When $T' \gtrsim T_\lambda$, the sample temperature was very stable when it was greater than T_λ, and increased only slowly when it was less than T_λ. During heat-capacity measurements for He II, T' generally was kept at T_λ

$+10^{-3}$ °K. For measurements on He I, T' was kept above T at all times.

During all heat-capacity measurements, the capillary temperature 5 cm above the bottom of the capillary vacuum was kept at about 50 °K. This was done in order to establish a very large density gradient near the bottom of the capillary, and to reduce the amount of helium not contained in the sample cell.

The heat-capacity measurements were made by a conventional technique. The bath temperature was reduced to the minimum attainable value (≈ 1.3 °K). Usually the platform temperature was adjusted so that, in absence of superfluid in the capillary ($T > T_\lambda$), the cell temperature was essentially constant with a given power dissipation in the thermometers. Alternately, the auxiliary heater could be used to establish this condition. When measurements were made for $T < T_\lambda$, the sample warmed up slowly because of superfluid flow in the capillary. The temperature-drift rate was established, and then power was dissipated in the main heater for a known length of time. After the heater power was turned off, the temperature drift was measured again. Under most circumstances the foredrift and afterdrift differed little from each other. An extrapolation to the middle of the heating-time interval was used to determined the temperature change.

The transition temperature was determined at the bottom of the probe. When the sample was heated through the transition, He I began to form first at this point because of the gravitational inhomogeneity[28] in the system. As soon as He I existed near the probe bottom, a temperature gradient developed across the probe and was detected with the differential thermometer (see Fig. 2 of Ref. 15). This transition temperature will be referred to as $T_{\lambda P}$, and could be determined with a precision of about 10^{-7} °K. From it, the transition temperature at the bottom of the main sample chamber ($T_{\lambda B}$) and at the sample surface ($T_{\lambda S}$) can be calculated.[28] All heat-capacity measurements were evaluated with respect to $T_{\lambda S}$.

D. Performance

1. *Thermometry*

The main thermometer bridge ratio changed by about 3×10^{-7} when the temperature near T_λ was changed by 10^{-6} °K. The bridge usually was operated with a power dissipation of 5×10^{-7} W in the thermometer, and under these circumstances the peak-to-peak noise in the ratio was approximately 1.5×10^{-7}, permitting a temperature resolution of about 10^{-7} °K (20% of the peak-to-peak noise). The self-heating of the thermometer was of the order to 500 °K/W. Thus, at the power level used for the measurements, the thermometer was warmer than the sample by 2.5×10^{-4} °K. In order to obtain a thermometer system which is as stable as the temperature resolution, it therefore is desirable to have a power supply which is stable at least over the time interval required to measure one heat-capacity point to one part in 2500. Using the HR-8 reference voltage, no instabilities due to changes in the thermometer self-heating have been observable over time intervals of about 1 h.

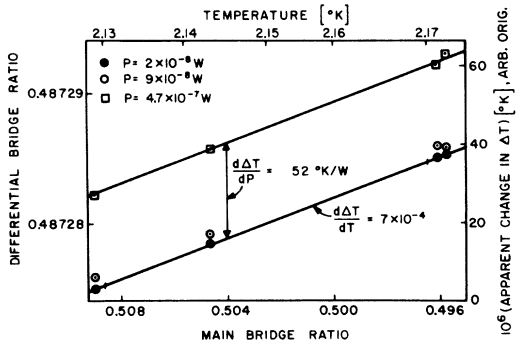

FIG. 7. Differential-thermometer bridge ratio as a function of the main thermometer bridge ratio.

The differential thermometer was about as sensitive to changes in temperature differences across the probe as the main thermometer was to changes in the temperature. It had a slightly larger resolution, since both resistive components were at low temperature,[28] and was less sensitive to changes in the absolute temperature than the main thermometer by over 3 orders of magnitude. This is demonstrated in Fig. 7, where the differential bridge ratio (or apparent temperature difference across the probe) is shown as a function of the main bridge ratio (or the absolute temperature) at three differential thermometer power levels for $T < T_\lambda$. It is also apparent from Fig. 7 that the self-heating is partially canceled in the differential system, and that the unbalance in the self-heating is smaller than the self-heating for the main thermometer by about 1 order of magnitude.

2. *Thermal Stability*

When the sample temperature was less than T_λ, there was of course a measurable heat input to the sample because of superfluid flow in the capillary. Under these circumstances, the heating rate of the sample was essentially independent of the temperature T' at the bottom of the capillary vacuum, provided T' was greater than T_λ. This has been discussed elsewhere.[32,33] Nonetheless, T' was kept constant to $\pm10^{-4}$ °K, and usually was equal to $T_\lambda + 10^{-3}$ °K. During the C_s measurements, heat transfer in the capillary was by He II film flow and was found to be given by[33]

$$\dot{Q}_f = 2.8\times10^{-3}(T_0 - T)^{1.4} \quad \text{for} \quad T_\lambda - T \lesssim 1.6\times10^{-2}\ ^\circ\text{K}\ , \tag{3}$$

with $\dot{Q}_f$ in watts and

$$T_0 = T_\lambda - 4\times10^{-4}\ ^\circ\text{K}\ .$$

Thus, under these circumstances the heat input from superfluid flow vanished below T_λ. Although we do not report in this paper the results of measurements of the heat capacity at constant volume C_v, we mention here that during the C_v measurements heat transfer in the capillary was by bulk He II, and is believed to be limited by the Gorter-Mellink mutual friction[32] between the normal fluid and the superfluid. In this case, experimental determinations of $\dot{Q}$[32] at relatively low pressure corresponded to

$$\dot{Q}_b = 0.012(T_\lambda - T)^{1.077} \quad \text{for} \quad T_\lambda - T \lesssim 10^{-3}\ ^\circ\text{K} \tag{4}$$

and

$$\dot{Q}_b = 0.0021(T_\lambda - T)^{0.821} \quad \text{for} \quad T_\lambda - T > 10^{-3}\ ^\circ\text{K}\ , \tag{5}$$

where $\dot{Q}_b$ is in watts. A few typical temperature-drift rates calculated from Eqs. (3)–(5) and the measured heat capacity are given in Table II. Over the temperature range of primary interest here ($|T_\lambda - T| \lesssim 10^{-2}\ ^\circ\text{K}$), $\dot{Q}_f$ and the corresponding foredrifts and afterdrifts during heat-capacity measurements were sufficiently small, and did not limit the precision of the measurements. At the lowest temperatures at which measurements of C_s were attempted ($T \cong 1.97\ ^\circ\text{K}$), the precision was limited by the film flow.

When the sample temperature was greater than the onset temperature for superfluidity, there was no superfluid flow, and the temperature stability was determined by the stability of other energy sources and the heat capacity of the sample. As mentioned previously, room-temperature radiation was virtually eliminated, and conduction was carefully controlled. However, in addition, there presumably was some energy input from vibration and radio-frequency heating which could not be controlled during the measurements. In order to investigate the constancy of these undesirable sources of power, the sample was heated to $(T_{\lambda P} + 5\times10^{-7})\ ^\circ\text{K}$. At this temperature, the lower half of the probe contains He I, and the rest of the sample consists of He II. The temperature difference across the probe with a differential thermometer power of about 10^{-7} W was then about $3\times10^{-5}\ ^\circ\text{K}$. This temperature difference depended strongly upon the height of the He I fraction,[15] and varied from 0 to about $6\times10^{-5}\ ^\circ\text{K}$ for a 1-cm change in this height, or a $10^{-6}\ ^\circ\text{K}$ change in the absolute temperature. Because of these circumstances, the differential thermometer could resolve changes in the absolute temperature of about $10^{-9}\ ^\circ\text{K}$ over a temperature range of about $10^{-6}\ ^\circ\text{K}$. Therefore, it was well suited for monitoring changes in power dissipation in the sample. It was observed that once the conduction heat leaks and the controllable power dissipation at the sample had been adjusted to result in immeasurably small temperature drifts, the sample temperature changed typically only by about $10^{-8}\ ^\circ\text{K}$ over a 1-h time period. It can be estimated that this corresponds to an average change in power dissipation of 0.4 ergs/min over a 1-h time interval.

TABLE II. The rate of change of the sample temperature due to superfluid flow in the capillary.

$T_\lambda - T$ (°K)	$10^6 dT/dt$ (° K/min) Film	Bulk
1×10^{-2}	2.0	12.8
5×10^{-3}	0.64	6.7
2×10^{-3}	0.13	2.8
1×10^{-3}	0.032	2.6
5×10^{-4}	0.002	1.1
2×10^{-4}	0.000	0.4

3. *Heat-Capacity Measurements*

Heat capacities were measured by adding a known amount of energy to the sample by means of the main heater, and observing the change in sample temperature with the main thermometer. The temperature change ΔT was determined from an extrapolation of the foredrift and the afterdrift of the sample temperature to the middle of the heating-time interval. For measurements on He II, the determination of ΔT presented no problem near T_λ where the drifts were small, because thermal equilibrium was fast and the thermometer response was limited only by the time constants in the measuring circuit (usually 3 sec). Measurements for He I were far more time-consuming because thermal equilibrium was attained only slowly after energy inputs. However, the thermal stability of the system was sufficient to permit waiting for equilibrium even for He I. A typical recorder-chart tracing for a heat-capacity measurement in He I about $4.6\times10^{-3}\ ^\circ\text{K}$ above T_λ is reproduced in Fig. 8. One can see that the sample container overheated appreciably during the energy input ($\approx10^{-4}\ ^\circ\text{K}$ at 2×10^{-4} W), and that about 15 min were required after the heating interval to establish thermal equilibrium. Nonetheless, it is evident that ΔT could be determined with a precision of about 0.1%. Very near T_λ, a much smaller heater power was used to reduce the overheating of the sample cell. Here, thermal equilibrium was faster than at higher temperatures, probably because of the larger thermal diffusivity of the sample[14,15] and more readily induced convection. A recorder trace of a series of five heat-capacity measurements which starts in

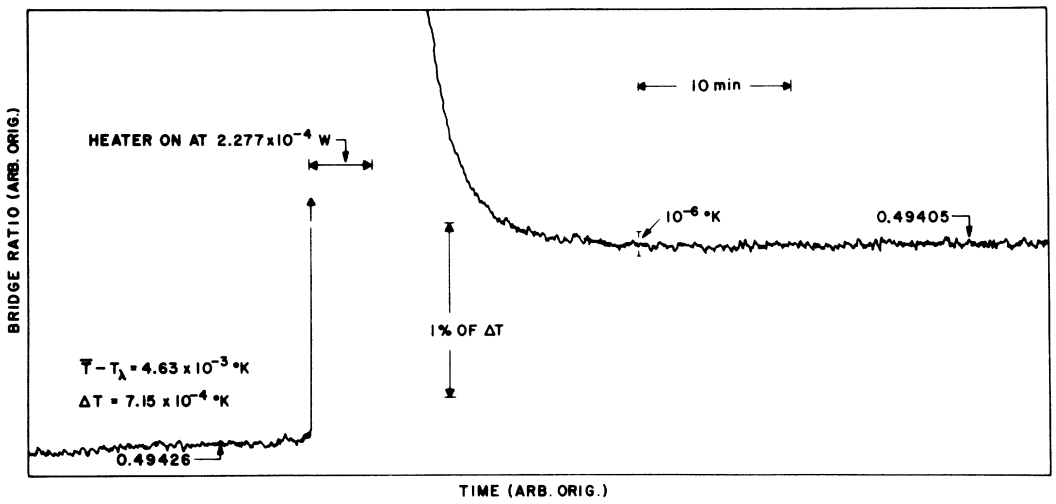

FIG. 8. A typical heat-capacity measurement for He I well above T_λ. Note that the bridge-ratio transformer setting, indicated in the figure, is different for the foredrift and afterdrift.

He II and ends in He I is shown in Fig. 9. The onset of thermal resistance of the sample is evident from a comparison of the afterdrifts for the 2nd and 3rd points. For these high-resolution measurements the precision of the results was limited by the temperature resolution of about 10^{-7} °K.

It should be mentioned that approximate thermal equilibrium also had to be attained in the probe, because the probe constituted about 1% of the sample mass. It is clear from work previously reported[14,15] that this was attainable. For the measurements reported here it was relatively easy to attain thermal equilibrium in the probe even for He I since heating was from the top, and heat transfer was largely by convection for temperatures less than that corresponding to the density maximum ($T_\lambda + 6 \times 10^{-3}$) °K. For higher temperatures, thermal equilibrium in the entire system was attained only after a considerably longer time period. For this reason, measurements for $T - T_\lambda > 6 \times 10^{-3}$ °K are not very plentiful.

At all times the temperature gradient across the

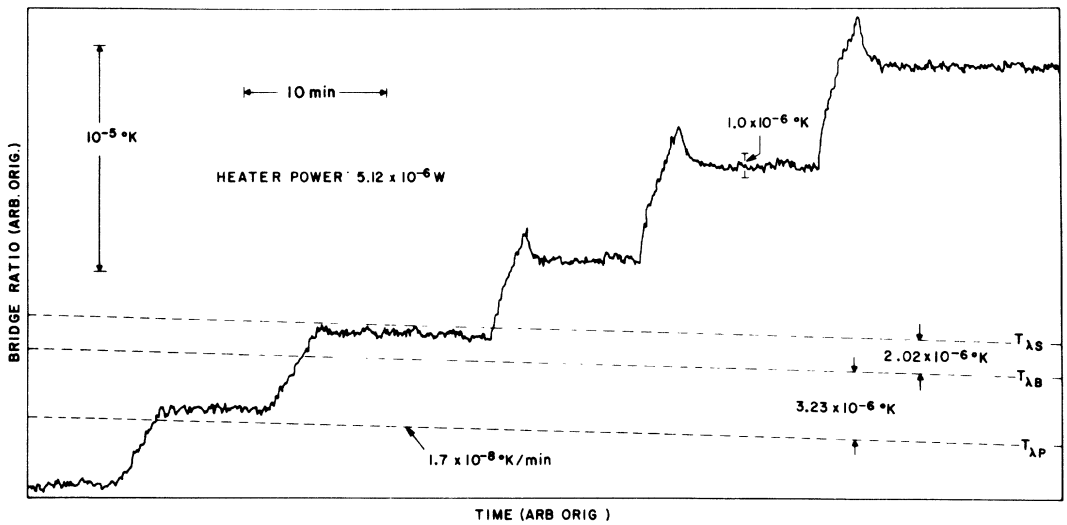

FIG. 9. Typical high-resolution heat-capacity measurements near T_λ. The transition temperatures at the bottom of the probe, the bottom of the main sample chamber, and the top of the sample are indicated by dashed lines. The nonhorizontal slopes of these lines correspond to the measured drift rate of the thermometer bridge ratio at constant temperature. The rapid thermal equilibrium for He II (first point) and the longer thermal time constants for He I (last three points) are apparent from the afterdrifts.

probe was kept small compared to $|T_\lambda - T|$ by reducing the differential-thermometer power, or by turning off the differential thermometer completely when not required.

III. DATA ANALYSIS

A. Corrections

The measured quantities are, at least in principle, not the desired thermodynamic variables C_s or C_p. Although the experiment was designed so as to minimize any deviations of the measurements from these thermodynamic functions, it is important either to demonstrate that these deviations are indeed negligible, or to apply appropriate corrections for them.

Experimental measurements yield the ratio $C_m = \Delta Q/\Delta T$, where ΔQ is the quantity of heat dissipated at the sample, and ΔT is the resulting temperature change. From this, it is necessary to derive the derivative

$$C = \lim_{\Delta T \to 0} C_m = \frac{dQ}{dT} . \tag{6}$$

This so-called curvature correction was applied in the usual manner,[41] and for most data points did not exceed 0.2% of C_m.

The heat capacity of the sample (C_t) is equal to the curvature corrected measured heat capacity C minus the heat capacity of the empty calorimeter C_E. From the weight of the cell (1189 g) and the known heat capacity of copper,[42] it was estimated that $C_E/C_t \lesssim 10^{-3}$. Further, C_E is regular at T_λ. Therefore, no correction was made for C_E.

During the measurements of C_s a small amount of vapor necessarily will be present in the sample cell. The measured heat capacity, therefore, will include, in addition to the heat capacity of the container and that of the liquid, also the heat capacity of the vapor present in the cell and the heat of vaporization required to maintain pressure equilibrium between liquid and vapor when the sample temperature is changed. The correction for this effect has been discussed by Hill and Lounasmaa,[43] and in more detail by Kellers.[2] It can be written in the form

$$C_s = (1-x)^{-1}\left\{\frac{C_t}{n} - x\left[\frac{L}{P}\left(\frac{\partial P}{\partial T}\right)_{S\,VP} - L\,\frac{n_l V_l}{n_g V_g}\,\alpha - \frac{2L}{T} + C_{pg}\right]\right\} , \tag{7}$$

where $x = PV_g/(nRT)$ and C_s is the desired molar heat capacity at saturated vapor pressure of the liquid. The total number of moles n of helium is determined experimentally. The vapor pressure P and its temperature derivative $(\partial P/\partial T)_{S\,VP}$ are taken from T_{58}.[38] The molar volume V_l and expansion coefficient at saturated vapor pressure $\alpha = V_l^{-1}(\partial V_l/\partial T)_{S\,VP}$ have been measured with sufficient accuracy by others.[37] The molar volume of the vapor is given by $V_g = RT/P + B$, where the second virial coefficient B can be adequately represented by[44]

$$B = 24 - 426/T \text{ cm}^3/\text{mole} , \tag{8}$$

and where R is the gas constant. The molar heat capacity at constant pressure of the vapor C_{pg}, although approximately equal to $\frac{5}{2}R$, is better represented by 21.44 J mole^{-1} °K^{-1}.[2,45] The number of moles of gas and vapor are given by

$$n_g = (V_c - nV_l)(B - V_l + RT/P)^{-1} \tag{9}$$

and $n_l = n - n_g$, respectively. Here V_c is the measured cell volume (81.53 cm^3). The heat of vaporization can be calculated from

$$L = T\left(\frac{\partial P}{\partial T}\right)_{S\,VP}\left(\frac{B - V_l + RT}{P}\right) . \tag{10}$$

The primary purpose of the work reported here is to obtain information about the singular contributions to C_p near T_λ. Inspection of Eq. (7) reveals that the difference between C_s and C_t diverges at T_λ because of the contribution from α. In addition, there are milder singularities in $C_s - C_t$ arising from $(\partial P/\partial T)_{S\,VP}$, L, and V_l. For this reason, the vaporization correction was applied to all data, although it was believed to be quite small. Later, it was observed that for the sample on which most of the conclusions from this work are based, the vaporization correction never exceeded 0.07% for $|t| \geq 10^{-4}$ °K and could have been neglected ($t \equiv T_\lambda - T$). For some other samples, however, it was larger.

For a system which is connected to an external volume by a capillary, an additional correction is required in principle for the energy used to vaporize sufficient sample to maintain the pressure in this external volume at saturated vapor pressure as the sample temperature is changed. It is difficult to calculate this correction because the temperature gradient along the capillary is not known in detail. Reasonable estimates show, however, that this correction does not exceed 0.01% of C_s for the present system.

The thermodynamic variable of primary interest is C_p. It can be shown that

$$C_p - C_s = TV_l\alpha\left(\frac{\partial P}{\partial T}\right)_{S\,VP} . \tag{11}$$

Near T_λ, the right-hand side of Eq. (11) can be evaluated from independent experimental data,[37,38] and

$$C_p - C_s \cong a_1 + b_1 \log_{10}|t| , \tag{12}$$

where

$$a_1 = 1.8 \times 10^{-3}, \quad b_1 = 1.2 \times 10^{-2} \quad \text{for} \quad T < T_\lambda \tag{13}$$

and

$$a_1 = 2.7 \times 10^{-2}, \quad b_1 = 1.2 \times 10^{-2} \text{ for } T > T_\lambda , \quad (14)$$

when the units of $C_p - C_s$ are J mole^{-1} °K^{-1}. Evaluation of Eq. (12) reveals that $C_p - C_s$ is always smaller than experimental errors in C_s (less than 0.07% for 10^{-4} °K $\leq |t| \leq 10^{-2}$ °K). Therefore, it was assumed for this work that $C_p = C_s$.

B. Errors

The errors in the final results are dominated by those arising from the determination of the sample mass m, the heat input ΔQ, and the temperature measurements. The sample mass is known with an accuracy of 0.2%, and systematic temperature-independent errors in C_s or C_v of this magnitude must be expected from this source. Both systematic and random errors in ΔQ are believed not to exceed 0.05%.

Errors arising from the thermometry introduce about the same absolute error into t and ΔT. Since t usually is greater than ΔT, it follows the relative errors in t are usually smaller than those in ΔT. If the specific heat has approximately the logarithmic functional form revealed by previous work,[1-5] then it can be shown that deviations of C_s from this function due to errors in t are smaller by at least a factor of 5 than deviations due to errors in ΔT. Therefore, errors in t may be neglected.

Systematic errors in ΔT are proportional to errors in dT/dR, where R is the thermometer bridge ratio. Uncertainties in dT/dR arise both from deviations of the working temperature scale from T_{58},[38] and from differences between T_{58} and the thermodynamic temperature. The effect of a 0.2% change in dT/dR upon the deviations $T - T_c$ of the thermometer calibration points from Eq. (2) is shown in Fig. 5 for the data of 8-7-68. It does not seem likely that systematic errors in ΔT (assuming T_{58} to be correct) are larger than this. Deviations of T_{58} from the thermodynamic temperature are difficult to estimate; but errors in ΔT from this source probably do not exceed 0.5%.[46]

From the above considerations it follows that the sum of all systematic errors in the heat capacity may be almost 1%. This is not particularly troublesome, since the temperature dependence of the heat capacity is of primary interest, and the absolute magnitude is relatively unimportant. One, therefore, should examine the temperature dependence of systematic errors in dT/dR with particular care. Over the temperature range of interest dT/dR is, within much less than 0.1%, a linear function of T. Further, it changes by only 0.3% of its value at T_λ when the temperature is changed by 10^{-2} °K. Comparison of several different analyses of the three thermometer calibrations in Fig. 5 indicate that the second derivative $d(dT/dR)/dT$ is known with an accuracy of at least 30%. Thus, it seems unlikely that systematic errors in ΔT change by more than 0.1% per 10^{-2} °K.

Near T_λ, random errors in ΔT are determined by the thermometer resolution of 10^{-7} °K. Sufficiently far from T_λ ($|t| \gtrsim 10^{-4}$ °K), ΔT was measured with a precision of 0.05–0.1% for the C_s measurements. In this region, the combined random errors in C_s arising from ΔT and ΔQ are about 0.1%. At temperatures very much less than T_λ ($t \gtrsim 10^{-1}$ °K) errors in ΔT for C_s increase again because of the large drift of the sample temperature.

C. Functional Form of C_p

For the analysis of the data in terms of theoretical models, it is convenient to use the dimensionless parameter

$$\epsilon \equiv t/T_\lambda = 1 - T/T_\lambda . \quad (15)$$

The corrected experimental measurements now consist of many pairs of numbers for C_p and ϵ. It is desired to derive from these data a few parameters which describe the entire set of measurements, and which can be compared with theoretical predictions. For this purpose, it is useful to adopt a trial function which relates C_p to ϵ. As is customary, we shall assume that C_p of a homogeneous system is asymptotically proportional to $|\epsilon|^{-\alpha}$, and write the specific heat in the form[47,48]

$$C_p \sim (A/\alpha)(|\epsilon|^{-\alpha} - 1) + B . \quad (16)$$

Equation (16) is assumed to be valid both for He I ($T > T_\lambda$) and He II ($T < T_\lambda$), but the parameters are allowed to assume different values in the two phases. In the limit as α vanishes, Eq. (16) becomes

$$C_p \sim -A \ln|\epsilon| + B . \quad (17)$$

Although the asymptotic behavior of divergent properties near critical points may be described appropriately by a power law such as $|\epsilon|^{-\alpha}$, it is well known that one must always expect correction terms of higher order. Fisher points out that, in the *simplest* case, these may take the form $|\epsilon|^{-\alpha}(1 + a\epsilon + \cdots)$.[48] However, there is no compeling reason why the higher-order terms should be expressible in this simple fashion. There are, in fact, some variables for which specific theoretical guidance about corrections to the asymptotic behavior is available, and where the correction terms are more complicated.[9,15] There is no rigorous theoretical information about higher-order contributions to the specific heat near T_λ, but we shall assume that these higher-order terms will take the form

$$D\epsilon \ln|\epsilon| + E\epsilon , \quad (18)$$

and present some arguments that indicate the reasonable nature of this form.

First, we consider the two-dimensional Ising model. In this case, rigorous information about the functional form of the heat capacity is available,[49] and although the superfluid transition may differ greatly from this model, a comparison seems worthwhile. The Ising-model specific heat in two dimensions can be written as an expansion about the transition temperature T_c, and has the form

$$C = -A\ln|\epsilon| + B + \sum_{i=1}^{\infty}(a_i\epsilon^i + b_i\epsilon^i\ln|\epsilon|)\,. \qquad (19)$$

The first two terms on the right-hand side of Eq. (19) correspond to Eq. (17), and those with $i=1$ have the form proposed in Eq. (18) for the corrections to the asymptotic behavior.

For further, and perhaps more convincing, evidence supporting Eq. (18), one can turn to thermodynamic arguments. We shall assume here that $\alpha = \alpha' = 0$ and consider the functional form of C_p along different experimental paths. Let us assume that C_p along an isobar diverges logarithmically near a λ line without higher-order contributions. Then it can be shown from thermodynamic arguments that the asymptotic divergence of C_p along any other path which meets the λ line at the same point as the isobar is also logarithmic and has the same amplitude (same A). But, in addition, C_p along the other path will contain higher-order terms, whose functional form depends upon the path. Along certain paths, for instance a path for which the pressure is proportional to ϵ, the higher-order terms will have the form of Eq. (18). Thus, if there are no higher-order terms in C_p, then this can at most be true along a specific path.

For further arguments, we compare C_p with other thermodynamic properties. It is known[34] that a pure logarithmic divergence of C_p (i.e., no higher-order terms) near a λ line requires that the isobaric thermal-expansion coefficient, whose asymptotic divergence will also be logarithmic, contain terms whose temperature dependence is ϵ and $\epsilon\ln|\epsilon|$. The same applies, for instance, to the isothermal compressibility.[34] Conversely, the *absence* of higher-order terms in the isobaric expansion coefficient or the isothermal compressibility requires that such terms be *present* in C_p. Unless there is some fundamental reason why the specific heat at constant pressure along a specific path occupies a special position among the divergent thermodynamic properties, it must therefore be expected that there are contributions to C_p which have the form of Eq. (18).

The above arguments are based upon the assumption that $\alpha = \alpha' = 0$. If this is not the case, but α and α' are small, then the correction terms in Eq. (18) should perhaps have a slightly, but probably not significantly, different form. We shall thus write the specific heat at constant pressure as

$$C_p \cong (A/\alpha)(|\epsilon|^{-\alpha} - 1) + B + D\epsilon\ln|\epsilon| + E\epsilon \quad \text{if } \alpha \neq 0 \qquad (20)$$

and as

$$C_p = -A\ln|\epsilon| + B + D\epsilon\ln|\epsilon| + E\epsilon \quad \text{if } \alpha = 0. \qquad (21)$$

We note further that the temperature dependence of $D\epsilon\ln|\epsilon| + E\epsilon$ over a limited experimental temperature range for $|\epsilon| \ll 1$ is very similar to that of ϵ.

Equations (20) and (21) are reasonable trial functions for C_p of a homogeneous liquid-helium sample near T_λ. However, the present measurements were made on a liquid with finite height in the earth's gravitational field. Such a system is not homogeneous, and there is a nonzero pressure gradient in the direction of its vertical axis.[28] Consequently, there is no unique transition temperature for the entire sample. There is, however, a local transition temperature $T_\lambda(h)$ for any depth h below the liquid surface. If Eq. (20) or (21) is valid locally in the sample, with ϵ dependent upon h, then the average (measured) C_p can be calculated by integrating Eq. (20) or (21) over h, and for $\alpha \neq 0$

$$\begin{aligned}\langle C_p\rangle = (A/\alpha)\{&\pm[aH(1-\alpha)]^{-1}\\ &\times(|\epsilon_s - aH|^{1-\alpha} - |\epsilon_s|^{1-\alpha}) - 1\}\\ &+ B + D\epsilon\ln|\epsilon| + E\epsilon\,,\end{aligned} \qquad (22)$$

where the positive sign is valid for He I, and the negative sign applies to He II. Here $\langle\ \rangle$ indicates the gravitational average, H is the total sample height, $\epsilon_s \equiv 1 - T/T_{\lambda s}$, and $T_{\lambda s}$ is the transition temperature at the surface of the sample. The parameter a is a property of the λ line, and at saturated vapor pressure has the value[28] 0.5861×10^{-6} cm^{-1}. For the case $\alpha = 0$, integration of Eq. (21) yields

$$\begin{aligned}\langle C_p\rangle = -A\{&\ln|\epsilon_s - aH| - 1 - [\epsilon_s/(aH)]\\ &\times\ln|(\epsilon_s - aH)/\epsilon_s|\}\\ &+ B + D\epsilon\ln|\epsilon| + E\epsilon\,.\end{aligned} \qquad (23)$$

In deriving these equations, the gravity effect on $D\epsilon\ln|\epsilon|$ and $E\epsilon$ was neglected because these terms contribute negligibly near T_λ. Equations (22) and (23) are suitable trial functions for the inhomogeneous sample encountered here, provided only the high-temperature (He I) or the low-temperature (He II) phase exists. However, over the temperature range from $T_{\lambda s}$ to $T_{\lambda s}(1 - aH)$ the two phases coexist. Over this range, the upper portion will consist of He II, and the lower portion will be He I. The two phases will have the heights

$$h_{II} = \epsilon_s/a; \quad h_I = H - \epsilon_s/a\,. \qquad (24)$$

Their heat capacities (per mole of the phase in question) are

$$\langle C_p\rangle_{\rm I} = \lim_{\epsilon_s \to 0} \langle C_p\rangle \tag{25}$$

and

$$\langle C_p\rangle_{\rm II} = \lim_{\epsilon_s \to aH} \langle C_p\rangle \ , \tag{26}$$

with $\langle C_p\rangle$ given by Eq. (22) or (23). The average heat capacity of the entire sample, considering the temperature-dependent contributions from the two single-phase fractions, then is given by

$$\langle C_p\rangle_{\rm I,II} = \frac{\epsilon_s}{aH}\left[\frac{A'}{\alpha'}\left(\frac{\epsilon_s^{-\alpha'}}{1-\alpha'} - 1\right) + B'\right] + 1 - \frac{\epsilon_s}{aH}\left[\frac{A}{\alpha}\left(\frac{(aH-\epsilon_s)^{-\alpha}}{1-\alpha} - 1\right) + B\right] \tag{27}$$

if α and α' differ from zero, and

$$\langle C_p\rangle_{\rm I,II} = (\epsilon_s/aH)\{-A'[\ln(\epsilon_s) - 1] + B'\} + (1 - \epsilon_s/aH) - A[\ln(aH-\epsilon_s) - 1] + B\} \quad \text{if } \alpha = \alpha' = 0. \tag{28}$$

In the temperature range where the two phases coexist, the higher-order terms may safely be assumed negligible. In the last two equations, the standard procedure[48] of identifying the parameters of the low-temperature phase by primed coefficients and those of the high-temperature phase by unprimed coefficients has been adopted.

D. Least-Squares Analysis

The best estimates for the parameters in Eqs. (22) and (23) and their standard errors can be computed from the data by a least-squares analysis in terms of these equations. In order to avoid undesirable effects from possible systematic differences between measurements performed on different samples, only results for the same sample were included in a given analysis. The data for He I were analyzed separately from those for He II, so that A, B, and α could be obtained independently of A', B', and α'. All data used in the analysis corresponded to measurements in the single-phase regions. Weights W inversely proportional to the square of the estimated random probable error[50] for each point were used. Specifically, the smaller of

$$W_i = (10^{-7}\Delta T^{-1} C_p)^{-2} \quad \text{and} \quad W_i = (10^{-3} C_p)^{-2} \tag{29}$$

for the ith data point was employed. Here 10^{-7} is the temperature resolution, and 10^{-3} corresponds to a probable error of 0.1%. A method of analysis employing polynominals which are orthogonal over the data points was used.

For simplicity, we shall neglect in this section the higher-order contributions to C_p, and discuss only the determination of A, B, and α. Then Eqs. (22) and (23) can be written in the form

$$\langle C_p\rangle = a + bf(\epsilon_s, \alpha) \ , \tag{30}$$

with $a = B$; $b = A/\alpha$ for $\alpha \neq 0$, and $a = B$; $b = -A$ for $\alpha = 0$. It was noted earlier that errors in ϵ_s are negligible compared to those in $\langle C_p\rangle$. Thus, a linear least-squares procedure which minimizes the estimate of the variance

$$\sigma^2 = \frac{N}{N-m-1}\sum_i W_i(\Delta C_p)_i^2 \Big/ \sum_i W_i \tag{31}$$

of C_p with respect to a and b may be employed if α is known.[50] Here $(\Delta C_p)_i$ is the deviation of $\langle C_p\rangle_i$ from Eq. (30) at the measured ϵ, N is the number of data points, and m is the number of parameters (3). Since α is *not* known, the minimum with respect to a and b of σ^2 was computed for several values of α in the vicinity of an initial guess for α. Whenever $\alpha = 0$ was used, Eq. (23) was employed to obtain $f(\epsilon_s, \alpha)$. For $\alpha \neq 0$, $f(\epsilon_s, \alpha)$ was based on Eq. (22). A typical example of σ as a function of α is given in Fig. 10. The best value of α, say α_0, is the one corresponding to the smallest value σ_0 of σ. The standard error of α is the absolute value of the difference between α_0 and the value of α corresponding to

$$\sigma = \sigma_0[1 + (N-m-1)^{-1}]^{1/2} \ . \tag{32}$$

If α were known, then the standard errors of a and b, and thus of A and B, could be obtained in the usual way[50] from the linear least-square fit. However, in order to obtain the true standard error of A and B, the correlation with α of A and B must be considered, and

$$\sigma_A = [(\sigma_A^{a,b})^2 + (\sigma_A^{\alpha})^2]^{1/2} \ , \tag{33}$$

where $\sigma_A^{a,b}$ would be the error in A if α were known, and σ_A^{α} is the change in A as α is changed from α_0 to $\alpha_0 + \sigma_\alpha$. An analogous equation pertains to σ_B.

IV. THEORETICAL PREDICTIONS

Recently developed theoretical ideas have led to a number of relations, called scaling laws, between the critical exponents which describe the asymptotic singularities of properties near critical points. In some cases even relations between the amplitudes of the leading singular terms are predicted. In this section we shall summarize those theoretical results which pertain to the present measurements. For a complete discussion, the reader is referred to the original literature,[22–27,30] and to a review article by Fisher.[48]

A fundamental assumption of the theory is that the Helmholtz free energy A of the system can be expressed as a function of an order parameter M and the temperature, and that the generalized "field" $H = (\partial A/\partial M)_T$ can be written in the form

$$H(\epsilon, M) = \mathrm{sgn}\{M\}|M|^{\delta} h(\epsilon/|M|^{1/\beta}) \ , \tag{34}$$

with h a homogeneous function of degree γ. Here δ and γ are critical exponents for various properties of the system, and are defined, for instance, in Ref. 24 or 48. There are some further restrictions upon h which follow from thermodynamic and other general considerations (see, e.g., Ref. 24 or 48). On the basis of these very general assumptions it can be shown that

$$\alpha = \alpha' . \tag{35}$$

If additional assumptions similar to those made about the free energy are also made about the correlation function for order-parameter fluctuations, then it follows that

$$\nu = \tfrac{1}{3}(2 - \alpha) , \tag{36}$$

$$\nu' = \tfrac{1}{3}(2 - \alpha') . \tag{37}$$

Here α and α' are defined by the asymptotic behavior of C_p given by Eqs. (16) and (17), and the coherence length ξ for fluctuations in the order parameter has the asymptotic form

$$\begin{aligned} \xi &\sim |\epsilon|^{-\nu} \text{ for } T > T_\lambda , \\ \xi &\sim |\epsilon|^{-\nu'} \text{ for } T < T_\lambda . \end{aligned} \tag{38}$$

An experimental value for ν' is available[25,7] from measurements of the superfluid density ρ_s [6-8] and the asymptotic proportionality between ρ_s and ξ^{-1} for $T < T_\lambda$.

In addition to the relations given by Eqs. (35)–(37) between exponents, scaling under some circumstances also results in explicit relations between the amplitudes of the asymptotic contributions to C_p above and below the transition. For a logarithmic divergence of C_p it is predicted[22-24] that

$$A = A' \text{ if } \alpha = \alpha' = 0 , \tag{39}$$

and for a finite C_p at T_λ one has[51]

$$B - A/\alpha = B' - A'/\alpha' \text{ if } \alpha = \alpha' < 0 . \tag{40}$$

Equation (40) implies that C_p, if it does not diverge, is continuous at T_λ.

The above discussion pertains to the singularities exhibited by static or equilibrium properties. It is known, however, that certain transport properties also diverge near critical points. Ferrell *et al.*[26] and Halperin and Hohenberg[27] have extended scaling arguments to transport properties by imposing certain homogeneity conditions upon the "critical frequencies" which describe the time-dependent fluctuations of certain properties. On the basis of this theory, Ferrell *et al.*[26] were able to predict that the thermal conductivity κ of He I near T_λ should diverge according to the power law

$$\kappa \sim \epsilon^{-x}; \quad x = 2\nu - \tfrac{3}{2}\nu' , \tag{41}$$

which in conjunction with Eq. (36) and (37) becomes

$$x = \tfrac{1}{3} - \tfrac{2}{3}\alpha + \tfrac{1}{2}\alpha' . \tag{42}$$

If Eq. (35) is also valid, then $x = \frac{1}{3}(1 - \frac{1}{2}\alpha)$. Thus, there is an additional opportunity to check the validity of a combination of scaling laws by comparing the singularity in C_p with that in κ.[14,15]

V. HEAT CAPACITY AT SATURATED VAPOR PRESSURE

A. Results

At saturated vapor pressure, the heat capacity was measured for two samples in the apparatus described in this paper. Only for one of these, to be called the main sample, were the measurements sufficiently extensive and precise to define adequately the limiting behavior of C_s near T_λ. Results for the other sample, to be called the auxiliary sample, will be used only in temperature regions where measurements for the main sample are lacking.

In addition, data had been obtained previously for $T < T_\lambda$ in a different apparatus on a sample which had a vertical height of 24.3 cm. The main features of these results have been mentioned briefly elsewhere.[28] However, further measurements have been made, and the data will be presented here in somewhat more detail. This sample will be referred to as the "tall" sample. Results for it are subject to a possible systematic error of 0.01 g or 0.6% in the sample mass. This error does not affect the temperature dependence of the measured heat capacity. Comparison with the results for the main sample did indeed indicate a small systematic difference, and the values of C_s reported here for the tall sample have been reduced from the original

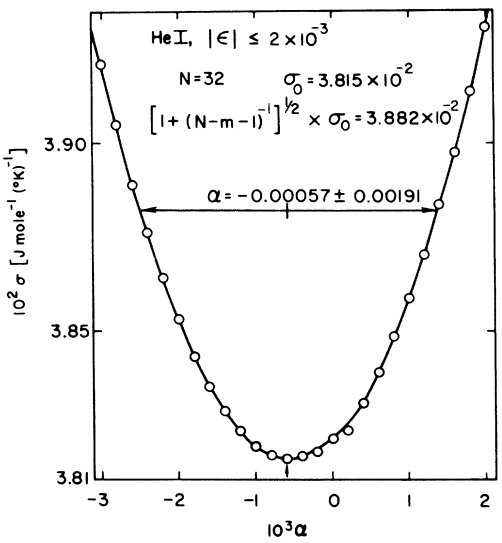

FIG. 10. The standard error σ as a function of α for a typical least-squares analysis.

estimate[28] by 0.6% in order to make them consistent with those for the main sample. In addition, it has been possible to apply more accurate vaporization corrections to the data, and to obtain a better estimate of the sample height than was previously available, because the sample container now has been taken apart, and direct measurements of its internal diameter have been made. For these reasons, the results to be quoted here differ slightly from those given previously.

The results for C_s near the transition for the main sample are presented in Table III. In this temperature range, the temperature increments ΔT used for the measurements are small, and for $\Delta T \leq 10^{-4}$ °K the temperature resolution limits the precision of C_s. For this reason, Table III includes all data for which $\Delta T \leq 10^{-4}$ °K, and ΔT is given with the data. The results further away from the transition are given in Table IV. For these data, ΔT is so large that it does not limit the precision, and random errors are believed to be about 0.1%. Tables III and IV include all data for the main sample which were used in the least-squares analyses to be discussed below.

Some of the results for the three samples are shown in Fig. 11 as a function of $\log_{10}|\epsilon_s|$ and $\log_{10}|T_{\lambda S} - T|$. Results for the tall sample were used only for large ϵ_s, where gravity effects are unimportant. Also shown are the measurements reported by Buckingham and Fairbank (BFK),[3] those by Hill and Lounasmaa (HL),[43] and the ones by Kramers, Wasscher, and Gorter (KWG).[52] The data by BFK are the averages of ten sets of mea-

TABLE III. Results of individual measurements of the heat capacity at saturated vapor pressure near T_λ. Data for which ΔT includes some of the two-phase region were omitted.

$10^6(T_{\lambda s} - T)$ (°K)	C_s (J mole^{-1} °K^{-1})	$10^6 \Delta T$ (°K)
14.5	76.0	5.0
9.8	78.0	4.9
5.6	83.5	3.9
−3.4	63.8	5.1
14.3	77.1	6.1
8.1	80.5	5.0
10.0	77.7	11.5
−3.2	65.3	4.0
18.4	75.9	20.3
5.0	82.8	4.5
19.0	74.0	27.4
7.0	81.9	4.1
−9.6	56.8	8.5
−6.5	58.0	4.8
6.5	82.2	3.8
2.4	86.8	3.9
−6.3	59.0	4.8
−11.4	57.1	5.1
−16.8	53.7	5.0
−17.9	54.6	30.4
−52.3	49.3	32.9
−88.3	46.4	33.8
−10.0	57.6	16.4
−37.1	51.0	32.2
−72.6	47.3	34.4
180.1	63.7	64.7
34.21	71.8	41.3

TABLE IV. Results of individual measurements of the heat capacity at saturated vapor pressure.

$10^4(T_{\lambda s} - T)$ (°K)	C_s (J mole^{-1} °K^{-1})	$10^4(T_{\lambda s} - T)$ (°K)	C_s (J mole^{-1} °K^{-1})
65.32	44.67	− 4.383	37.78
61.99	44.92	− 6.855	35.41
58.62	45.25	− 10.25	33.22
55.20	45.54	− 13.78	31.63
51.69	45.93	− 17.24	30.43
48.27	46.27	− 20.69	29.46
41.55	47.07	− 24.14	28.64
38.17	47.60	− 27.53	27.93
34.78	48.06	− 30.80	27.33
31.36	48.61	− 34.04	26.80
27.92	49.23	− 1.728	42.75
24.60	49.88	− 5.097	36.98
21.27	50.65	− 11.84	32.50
17.56	51.71	− 18.78	29.99
14.17	52.85	− 30.14	27.48
10.83	54.28	− 39.49	26.04
7.495	56.20	− 46.31	25.20
4.973	58.32	− 53.39	24.44
2.885	61.05	− 60.48	23.77
1.282	65.28	43.72	46.86
17.21	51.84	36.89	47.79
15.56	52.28	30.33	48.86
13.89	52.93	17.25	51.79
12.22	53.58	10.71	54.28
10.55	54.44	4.739	58.46
8.881	55.22	1.220	65.51
7.197	56.36	158.9	39.48
10.08	54.60	141.9	39.76
8.392	55.56	108.4	41.76
6.708	56.72	91.59	42.76
5.030	58.30	74.95	43.89
3.348	60.31	58.26	45.30
1.685	63.88	46.49	46.52
4.865	58.34	26.27	49.61
3.178	60.50	19.57	51.12
1.215	65.37	12.86	53.32
− 2.379	41.08	6.244	57.03
5.175	57.97	2.168	62.40
3.533	60.04	357.2	34.04
1.850	63.29	320.2	34.94
− 0.895	46.14	277.3	35.89
− 2.660	40.43	240.3	36.97
168.1	39.17		
100.0	42.30		
66.60	44.60		
14.82	52.60		
11.53	54.02		
7.972	55.92		
4.482	58.98		

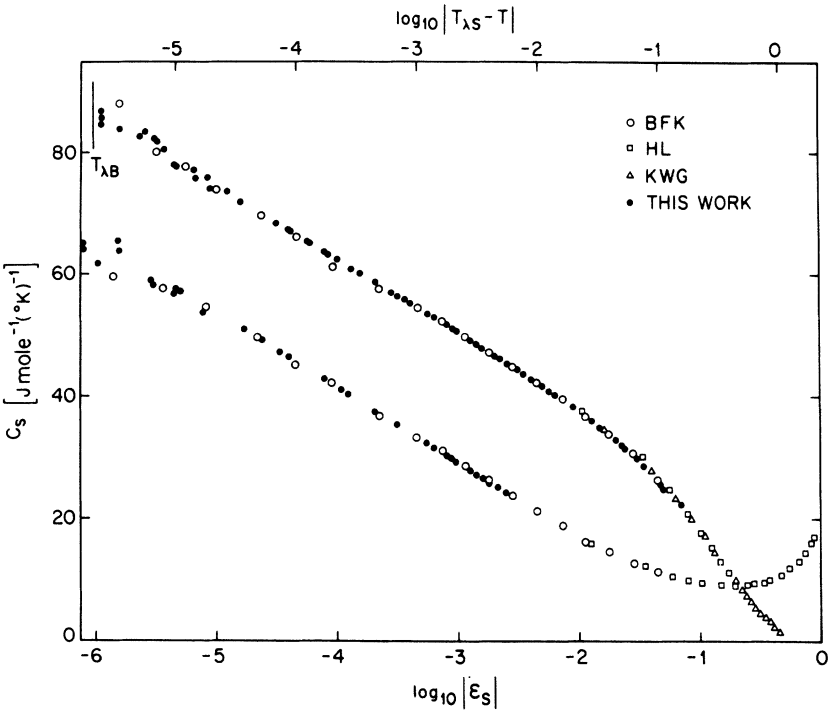

FIG. 11. The heat capacity at saturated vapor pressure as a function of $\log_{10}|\epsilon_s|$ and $\log_{10}|T_{\lambda S}-T|$. The transition temperature at the bottom of the sample is indicated in the upper left corner: open circles, Ref. 3; squares, Ref. 43; triangles, Ref. 52; solid circles, this work.

surements, and thus do not reflect fully the scatter of individual measurements. The transition temperature $T_{\lambda B}$ at the bottom of the main and auxiliary sample is indicated near the upper left corner of the graph. The sample of BFK was of about the same height, and thus has the same $T_{\lambda B}$. The values of $T_\lambda - T$ quoted by BFK are based on the assumption that C_s reaches a maximum at T_λ. It is now evident that C_s is a maximum at $T_{\lambda B}$. Therefore, the BFK values of $T_\lambda - T$ were adjusted by 2×10^{-6} °K to obtain $T_{\lambda S} - T$. It is clear from Fig. 11 that the agreement between the four sets of measurements is good, and that any systematic differences between them are smaller than the resolution of this graph.

The available data very near the transition are shown in Fig. 12 as a function of $T_{\lambda S} - T$. The solid squares correspond to the measurements given in detail in Fig. 9. Also shown are results near T_λ reported by Fairbank and Kellers.[5] These data correspond to individual measurements taken during a single successful "run." $T_{\lambda S}$ was adjusted so that the largest reported value of C_s occurs at $T_{\lambda B}$. In addition, the appropriate curvature correction was applied to the values of C_s given in Ref. 5. There-

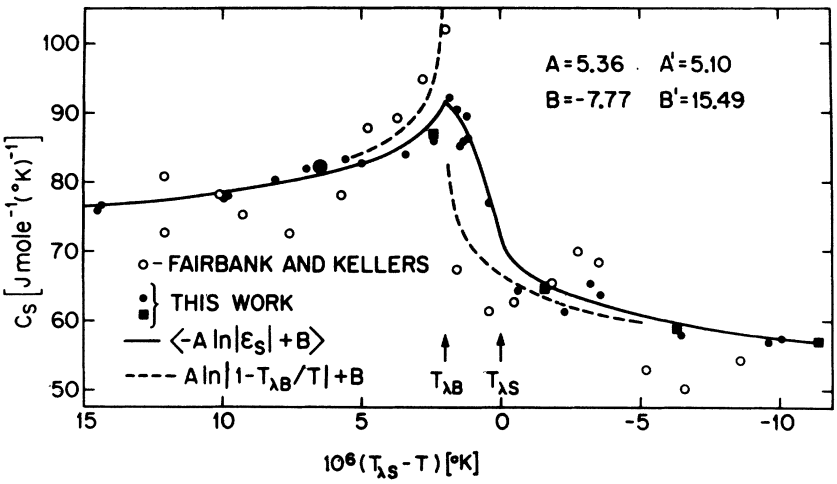

FIG. 12. The heat capacity at saturated vapor pressure near the transition as a function of $T_{\lambda S} - T$: open symbols, Ref. 5; solid symbols, this work. The solid squares correspond to the measurements shown explicitly in Fig. 9. The solid line corresponds to the gravity average of the logarithmic divergence for the homogeneous system. The dashed line is the logarithmic divergence expected for the homogeneous system. This latter curve was positioned along the temperature axis so that its maximum coincides with the measured specific-heat maximum ($T_\lambda = T_{\lambda B}$).

fore, the results as shown here should no longer reflect the rounding which results from averaging over a finite temperature interval, which is indicated in Fig. 6 of Ref. 5. The solid line in Fig. 12 corresponds to Eqs. (23) and (28), with the parameters determined by a least-squares analysis which included data much further from $T_{\lambda S}$. For comparison, Eq. (21) with the same parameters (no gravity) is shown as a dashed line. For this curve, however, T_λ was chosen as $T_{\lambda B}$ so that the temperature for the maximum of this curve coincides with that for the true specific-heat maximum. The present measurements agree well with the gravity corrected expressions Eqs. (23) and (28), and differ considerably from Eq. (21) which neglects gravity. The scatter in the earlier measurements[5] is larger, and they appear reasonably consistent with either functional form.

B. Analysis and Discussion

All parameters to be quoted in the remainder of this paper are with reference to the heat capacity in the units J mole^{-1}(°K)$^{-1}$. The determination of the parameters A, B, α, A', B', and α' would be relatively simple if it could be assumed that the higher-order terms $D\epsilon \ln|\epsilon| + E\epsilon$ make a negligible contribution to C_p for $|\epsilon|$ less than same value, say ϵ_{max}, which lies well inside the experimentally accessible temperature range. Initially, this assumption was made, and it was found that for $\epsilon_{max} \leq 3 \times 10^{-3}$ the data for the main sample yield

$$\begin{aligned} &\alpha = 0.000 \pm 0.003; && \alpha' = -0.020 \pm 0.003 , \\ &A = 5.355 \pm 0.15; && A' = 6.081 \pm 0.15 , \\ &B = -7.773 \pm 0.5; && B' = 11.345 \pm 0.5 , \end{aligned} \tag{43}$$

with α and α' independent of ϵ_{max} within their standard errors.[29] It is apparent that α and α' do not satisfy the scaling prediction, Eq. (35). Since $\alpha' \neq 0$, Eq. (39) does not apply. From Eqs. (36) and (37) one obtains $\nu' = 0.673 \pm 0.001$ and $\nu = 0.666 \pm 0.001$. Direct measurements of ρ_s[6–8] yield $\nu' = 0.666 \pm 0.006$, differing only by one standard error from the present estimates. The thermal conductivity of He I diverges asymptotically with an exponent $x = 0.334 \pm 0.005$.[14,15] The above analysis of C_p and Eq. (42) give 0.323 ± 0.003. In this case, the difference is 1.4 times the sum of the standard errors, and cannot be regarded as significant. Thus, the only violation of scaling laws which results from this analysis is the result $\alpha \neq \alpha'$. This, however, would appear to be a rather serious breakdown of the theory.

{ *Note added in proof.* Recent more precise measurements of the thermal conductivity κ [G. Ahlers, in Proceedings of the Twelfth International Conference on Low Temperature Physics, Kyoto, Japan. (unpublished)] have revealed that 0.334 is not the asymptotic exponent for κ, and that higher-order terms make sizable contributions to κ for $\epsilon \geq 10^{-5}$. It is now clear that $x \neq \frac{1}{3}$, in violation of Eqs. (41) and (42).}

One might be tempted to believe that the temperature independence of α and α' for $\epsilon_{max} \leq 3 \times 10^{-3}$ supports the assumption that higher-order contributions to C_p are negligible in this range. However, this is not justified, expecially since α and α' are temperature independent only within their probable errors, and since these errors diverge as ϵ_{max} vanishes. Therefore, it is necessary to investigate possible effects of higher-order contributions upon α and α'. As pointed out above, there is no reliable theoretical guidance about the form of higher-order contributions to C_p. We were able only to present arguments which lead to Eq. (18) as a reasonable form for these terms, but more complicated terms have not been rigorously excluded. Therefore, it does not seem very fruitful to carry out a detailed analysis of the data in terms of the complete Eqs. (22) and (23). If such an analysis were carried out, it would involve the determination of five parameters for each phase, and the correlation between the parameters would result in large probable errors such that $\alpha = \alpha'$ would be included in the results. Even if it were not, one would still be at liberty to postulate more complicated contributions. We shall take a somewhat simpler approach to the problem, and approximate the contributions postulated in Eq. (18) by $E_1'\epsilon$ and $E_1\epsilon$ for small ϵ. On the basis of this functional form, the values $\alpha \cong -0.005 \pm 0.005$ and $\alpha' \cong -0.015 \pm 0.007$ were obtained. These results reasonably permit the specific values

$$\begin{aligned} &\alpha' = \alpha = -0.009 , \\ &A' = 5.504 , && A = 5.820 , \\ &B' = 13.85 , && B = -9.90 , \\ &E_1' \cong E_1 \cong -120 . \end{aligned} \tag{44}$$

These parameters satisfy the scaling prediction $\alpha = \alpha'$ [Eq. (35)]. Since $\alpha \neq 0$, Eq. (39) does not apply. Further, we note that $E_1' = E_1$ indicates that higher-order contributions, although appreciable in the temperature range of interest, are regular at T_λ. The derived exponents $\nu' = 0.670$ and $2\nu - \frac{3}{2}\nu' = 0.335$ are in very good agreement with the more direct determinations (0.666 ± 0.006)[6–8] and $(0.334 \pm 0.005$[14,15]) (see Note added in proof above). This interpretation appears to be in agreement with scaling predictions. However, $\alpha = \alpha' < 0$ implies that C_p, although singular at T_λ, does not diverge at T_λ.

For the case $\alpha = \alpha' < 0$, there is the additional scaling prediction given by Eq. (40). It is difficult to test this prediction on the basis of the parameters

in Eq. (44) because $B - A/\alpha$ is a rapidly varying function of α. Therefore, the difference $(B - A/\alpha) - (B' - A'/\alpha')$ with $\alpha = \alpha'$ was computed for several values of α, and was found to vary between 21 and 6 J mole^{-1} °K^{-1} when α was changed from -0.007 to -0.011, and its probable error was found to be equal to 3 when $\alpha = \alpha' = -0.009$. Thus, it follows that only $\alpha = \alpha' < -0.009$ would be consistent with Eq. (40). Although it appears that the measurements, within their possible errors, are not totally inconsistent with Eq. (40), it does appear that the agreement is not particularly good.

We shall attempt now to determine whether the measurements are also consistent with $\alpha = \alpha' = 0$ and the form postulated in Eq. (18) for higher-order contributions. In this case, according to the original formulation of scaling, the divergent contribution to C_p is symmetric about T_λ. Therefore, we shall examine the difference

$$\Delta C = C_p - \langle -A_0 \ln|\epsilon| + B_0 \rangle$$

between the measured heat capacity C_p and the gravity averaged expression for C_p based upon the parameters A_0 and B_0 for He I. The subscripts on A and B indicate that $\alpha \equiv 0$ is assumed. If there is a value of ϵ_{max} below which Eq. (23) adequately describes the He II measurements ($\alpha' = 0$), then ΔC for $T < T_\lambda$ should be linear in $\log_{10}(\epsilon_s)$ for sufficiently small ϵ_s. Values of ΔC, obtained with A_0 and B_0 in Eq. (43), already were presented in Ref. 30. It was seen that $\alpha' = 0$ is consistent with the data for $\epsilon_s \lesssim 3 \times 10^{-4}$. However, $\alpha' = 0$ implies that higher-order terms begin to contribute appreciably for He II when $\epsilon_s \cong 3 \times 10^{-4}$. For He I these terms are negligible for $\epsilon_s \lesssim 3 \times 10^{-3}$ if $\alpha = 0$. Thus, $\alpha = 0$ and the scaling prediction $\alpha = \alpha'$ are consistent with the data, but appear to imply a severe asymmetry in higher-order contributions.

TABLE V. Parameters for the logarithmic divergence of C_p obtained for several values of the maximum $|\epsilon|$ at which data were used. The quoted standard errors do *not* include contributions from higher order terms.

$\log_{10}(\epsilon_{max})$	A_0'	B_0'
−3.5	5.109 ± 0.038	15.43 ± 0.33
−3.4	5.102 ± 0.028	15.49 ± 0.24
−3.3	5.117 ± 0.021	15.36 ± 0.18
−3.2	5.122 ± 0.019	15.31 ± 0.16
−3.0	5.155 ± 0.014	15.03 ± 0.12
−2.8	5.176 ± 0.012	14.85 ± 0.10
−2.6	5.211 ± 0.011	14.56 ± 0.08
	A_0	B_0
−3.3	5.347 ± 0.017	− 7.71 ± 0.15
−3.0	5.357 ± 0.010	− 7.79 ± 0.08
−2.7	5.355 ± 0.006	− 7.77 ± 0.05
−2.5	5.347 ± 0.006	− 7.71 ± 0.04

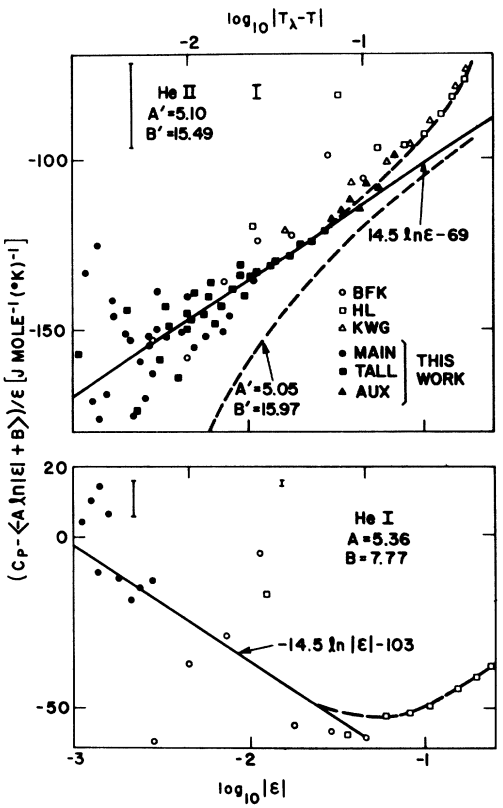

FIG. 13. Deviations of C_s for large ϵ from the asymptotic logarithmic divergence, multiplied by ϵ^{-1}. A straight line on this graph implies higher-order contributions to C_p of the form $D\epsilon \ln|\epsilon| + E\epsilon$. The error bars indicate the effect of a 0.1% change in C_p.

The scaling assertion $A_0 = A_0'$ [Eq. (39)] requires that ΔC for He II be independent of ϵ when higher-order contributions are negligible. Even for $\epsilon_{max} < 3 \times 10^{-4}$, where $\alpha' = 0$ is consistent with the data, the measured ΔC is temperature dependent.[30] Thus, $A_0 \neq A_0'$, in contradiction to Eq. (39). The data yield $A_0' < 5.13$ for $\epsilon_{max} \lesssim 5 \times 10^{-4}$. Thus,

$$A_0/A_0' > 1.041 \quad \text{if} \quad \alpha = \alpha' = 0 . \tag{45}$$

It does not seem likely that A_0/A_0' exceeds 1.06. The most reasonable values for the parameters are $A_0' = 5.10$ and $B_0' = 15.52$.

In order to demonstrate more explicitly on the basis of numerical analyses of the data that $A_0 > A_0'$, we have obtained values of A_0, B_0, A_0', and B_0' by fitting the data for which $|\epsilon|$ is less than ϵ_{max} to Eq. (23); but in this analysis we have neglected the higher-order terms of the form $\epsilon \ln|\epsilon|$ and ϵ. The results for the coefficients for several ϵ_{max} are given in Table V. These results lead to the same conclusions, Eq. (45), as the graphical analysis.

We shall now examine the temperature dependence

of higher-order contributions implied by the last analysis ($\alpha = \alpha' = 0$). Particularly, it will be interesting to see if the temperature dependence of these terms is indeed consistent with Eq. (18). For this purpose, we shall investigate the validity of Eq. (23), and rewrite it in the form

$$(C_p - \langle -A_0 \ln|\epsilon| + B_0 \rangle)/\epsilon = D_0 \ln|\epsilon| + E_0 \qquad (46)$$

for He I. The equivalent expression with primed coefficients pertains to He II. The experimental results corresponding to the left-hand side of this equation are shown as a function of $\log_{10}|\epsilon|$ in Fig. 13. Also shown are the results of BFK,[1-5] HL,[43] and KWG.[52] It is apparent that the results for He II are of the form given by Eq. (23) for $\epsilon \lesssim 5\times10^{-2}$. For larger ϵ, one can reasonably expect additional terms not included in Eq. (23). The experimental information for He I is not as plentiful, but all available data are consistent with $D_0' \cong -D_0 \cong 14.5$, $E_0' \cong -69$, and $E_0 \cong -103$, as shown by the solid lines in Fig. 13. The average effect upon the data for He II in this figure of a 1% change in A_0' is shown as a dashed line. It is apparent that a larger change in A_0' would no longer be consistent with the assumed functional form for higher-order contribution. We see that the contribution with temperature dependence $\epsilon \ln|\epsilon|$ is approximately symmetric about T_λ, and that the ϵ contribution is asymmetric. For He I, the two contributions are of opposite sign, and within experimental error cancel each other for $\epsilon \lesssim 3\times10^{-3}$. For this reason, there appeared to be no higher-order contributions to C_p for He I.

Through the above analysis of the data, it was possible to show that the results of this work are quite consistent with $\alpha = \alpha' = 0$. In addition, it is apparent that the higher-order terms implied by the data and $\alpha = \alpha' = 0$ are of the expected functional form, and are to some extent symmetric about $T_\lambda(D_0 \cong -D_0')$. However, there appears to be no compelling theoretical reason at this time why a symmetry in higher-order contributions should exist, and we do not at present attach any particular sig-

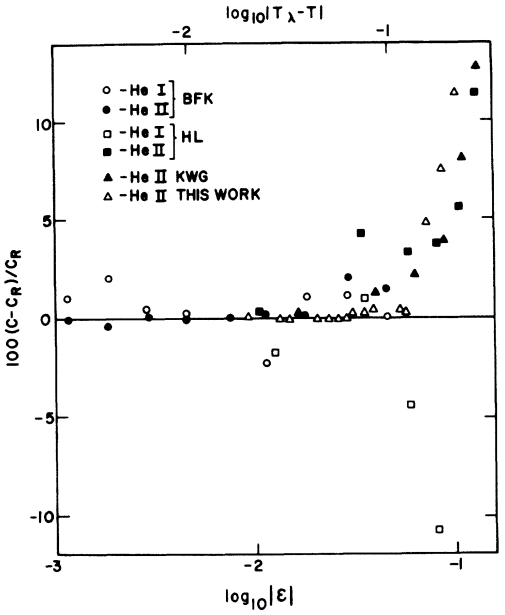

FIG. 15. Deviations in percent at large ϵ of C_s from the adopted functional form of C_s. Data are from Ref. 3, circles; Ref. 43, squares; Ref. 52, solid triangles; and this work, open triangles.

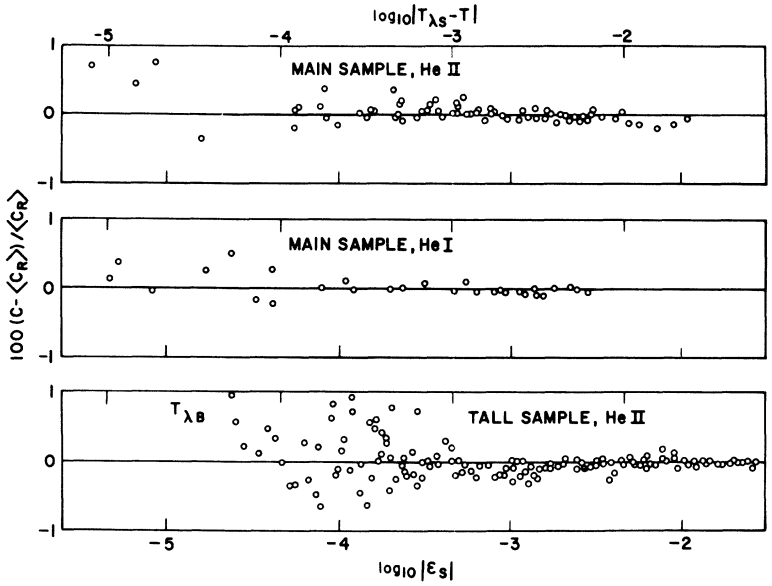

FIG. 14. Deviations in percent of the measured C_s from the adopted functional form for C_s, Eq. (48).

nificance to the observation that $D_0 \cong -D_0'$ at saturated vapor pressure.

For the purpose of thermodynamic calculations, it is desirable to have an analytic representation of the measurements. From the three interpretations of the data given in this section, we choose the case $\alpha = \alpha' = 0$ for this purpose, and summarize the results:

$$C_p = -A_0\langle \ln|\epsilon_s|\rangle + B_0 + D_0\epsilon \ln|\epsilon| + E_0\epsilon \ , \qquad (47)$$

with

$$\begin{aligned} A_0 &= 5.355 \pm 0.01, & A_0' &= 5.100^{+0.03}_{-0.05}, \\ B_0 &= -7.773 \pm 0.1, & B_0' &= 15.52^{+0.45}_{-0.28}, \\ D_0 &= -14.5, & D_0' &= 14.5, \\ E_0 &= -103, & E_0' &= -69, \end{aligned} \qquad (48)$$

where the units of C_p are J mole^{-1} °K^{-1}. The errors quoted for A_0, B_0, A_0', and B_0' do not include possible systematic errors in C_p, and are based upon the assumption that the functional form of Eq. (47) is valid. The errors result primarily from the correlation between A and B. Over the range indicated by the errors, A_0 and A_0' are approximately linear functions of B_0 and B_0'. Therefore, any change in A_0 or A_0' should be accompanied by a corresponding change in B_0 and B_0'. Specifically, A_0 and B_0 or A_0' and B_0' should be varied over the indicated ranges only with the constraint

$$dA_0/dB_0 \cong dA_0'/dB_0' \cong -0.11 \ . \qquad (49)$$

In order to show the precision with which the measurements can be represented by Eqs. (47) and (48), the deviations from it of the data in percent are shown in Fig. 14. For larger $|\epsilon|$, the deviations from this equation of measurements from all available sources are shown in Fig. 15. It is apparent that these deviations approach about 1% only when $|\epsilon|$ is as large as 5×10^{-2}.

VI. SUMMARY

In this paper, a detailed description of an apparatus and of procedures for the precision measurement of several properties of liquid helium near T_λ are presented and the performance of the equipment is evaluated. Measurements of the heat capacity at saturated vapor pressure are reported. From these results, the heat capacity at constant pressure is derived, and discussed in terms of current critical-point theories. The interpretation in terms of the asymptotic temperature dependence $C_p \sim |\epsilon|^{-\alpha}$ is difficult because of possible contributions to C_p for $|\epsilon| > 0$ from terms of higher order than the dominating asymptotic contribution. For this reason, three possible interpretations are given. If higher-order contributions to C_p are neglected for $|\epsilon| \lesssim 3\times10^{-3}$, then the data imply $\alpha' < 0$ and $\alpha = 0$. This is contrary to theoretical predictions. If higher-order terms are considered, then $\alpha = \alpha' < 0$ is consistent with the data. Although agreement with theoretical predictions can be obtained with this analysis, the results imply that C_p is finite at T_λ. As a third alternative, $\alpha = \alpha' = 0$ can also be obtained if enough flexibility is allowed in the postulated higher-order terms; however, this last interpretation results in unequal amplitudes of the asymptotic divergence above and below T_λ. Current theory requires that the amplitudes be equal if $\alpha = \alpha' = 0$. It is apparent that it would be desirable to reexamine the theory in order to see if reasonable modifications can be made which would permit unequal amplitudes even if $\alpha = \alpha' = 0$. An attempt at modifying the theory so as to attain agreement with the present results has been made by Fisher.[29]

Note added in proof. Measurements of the heat capacity under pressure [G. Ahlers, in Proceedings of the Twelfth International Conference on Low Temperature Physics, Kyoto, Japan (unpublished)] have revealed that C_p at 7 and 15 bar can be described by $\alpha = \alpha' = 0 \pm 0.005$, and that higher-order terms at these pressures do not contribution appreciably for $\epsilon \lesssim 3\times10^{-3}$. These measurements still yield $A/A' > 1$. Recent measurements of C_s for He^4 by F. Gasparini and M. R. Moldover [Phys. Rev. Letters 23, 749 (1969)] also tend to support $A/A' > 1$ at vapor pressure if $\alpha = \alpha' = 0$.

[1]W. M. Fairbank, M. J. Buckingham, and C. F. Kellers, in *Proceedings of the Fifth International Conference on Low Temperature Physics and Chemistry*, edited by J. R. Dillinger (University of Wisconsin Press, Madison, Wisc. 1958), p. 50.

[2]C. F. Kellers, Ph. D. thesis, Duke University, Durham, N. C., 1960 (unpublished).

[3]M. J. Buckingham and W. M. Fairbank, in *Progress in Low Temperature Physics*, edited by C. J. Gorter (North-Holland, Amsterdam, 1961), Vol. III, p. 80.

[4]W. M. Fairbank, in *Proceedings of the International School of Physics "Enrico Fermi"*, Course XXI, edited by G. Careri (Academic, New York, 1963), p. 293.

[5]W. M. Fairbank and C. F. Kellers, in *Critical Phenomena, Proceedings of a Conference*, edited by M. S. Green and J. V. Sengers Natl. Bur. Std. Misc. Pub. No. 273 (U.S. GPO, Washington, D.C., 1966), p. 71.

[6]J. R. Clow and J. D. Reppy, Phys. Rev. Letters 16, 887 (1966).

[7]J. A. Tyson and D. H. Douglass, Jr., Phys. Rev. Letters 17, 472 (1966).

[8]J. A. Tyson, Phys. Rev. 166, 166 (1968).

[9]C. J. Pearce, J. A. Lipa, and M. J. Buckingham, Phys. Rev. Letters 20, 1471 (1968).

[10]J. A. Tyson and D. H. Douglass, Jr., Phys. Rev. Letters 21, 1308 (1968).

[11]D. L. Johnson and M. J. Crooks, Phys. Letters 27A, 688 (1968).
[12]R. Williams, S. E. A. Beaver, J. C. Fraser, R. S. Kagiwada, and I. Rudnick, Phys. Letters 29A, 279 (1969).
[13]D. L. Johnson and M. J. Crooks, Phys. Rev. 185, 253 (1969).
[14]G. Ahlers, in *Proceedings of the Eleventh International Conference on Low Temperature Physics*, edited by J. F. Allen, D. M. Finlayson, and D. M. McCall (University of St. Andrews Printing Department, St. Andrews, Scotland, 1968), p. 203.
[15]G. Ahlers, Phys. Rev. Letters 21, 1159 (1968).
[16]J. A. Tyson, Phys. Rev. Letters 21, 1235 (1968).
[17]C. E. Chase, Phys. Fluids 1, 193 (1958).
[18]M. Barmatz and I. Rudnick, Phys. Rev. 170, 224 (1968).
[19]W. Heinicke, G. Winterling, and K. Dransfeld, Phys. Rev. Letters 22, 170 (1969).
[20]J. S. Imai and I. Rudnick, Phys. Rev. Letters 22, 694 (1969).
[21]G. Ahlers, Phys. Letters 28A, 507 (1969).
[22]B. Widom, J. Chem. Phys. 43, 3892 (1965); 43, 3898 (1965).
[23]L. P. Kadanoff, Physics 2, 263 (1966).
[24]R. B. Griffiths, Phys. Rev. 158, 176 (1967).
[25]B. D. Josephson, Phys. Letters 21, 608 (1966).
[26]R. A. Ferrell, N. Ményhard, H. Schmidt, F. Schwabl, and P. Szépfalusy, Phys. Rev. Letters 18, 891 (1967); Phys. Letters 24A, 493 (1967); Ann. Phys. (N. Y.) 47, 565 (1968).
[27]B. I. Halperin and P. C. Hohenberg, Phys. Rev. Letters 19, 700 (1967); Phys. Rev. 177, 952 (1969).
[28]G. Ahlers, Phys. Rev. 171, 275 (1968).
[29]M. E. Fisher, as quoted in Ref. 30.
[30]G. Ahlers, Phys. Rev. Letters 23, 464 (1969).
[31]G. Ahlers, Bull. Am. Phys. Soc. 12, 374 (1967).
[32]G. Ahlers, Phys. Rev. Letters 22, 54 (1969).
[33]G. Ahlers, J. Low Temp. Phys. 1, 159 (1969); Bull. Am. Phys. Soc. 14, 417 (1969).
[34]G. Ahlers, Phys. Rev. 182, 353 (1969).
[35]The measurements presented in Refs. 14 and 15 were made in this probe.
[36]The measurements presented in Refs. 32 and 33 were made in the section of this capillary between the bottom of the capillary vacuum and the sample cell.
[37]E. C. Kerr and R. D. Taylor, Ann. Phys. (N. Y.) 26, 292 (1964).
[38]H. van Dijk, M. Durieux, J. R. Clement, and J. K. Logan, Natl. Bur. Std. (U. S.) Monograph No. 10 (U. S. GPO, Washington, D. C., 1960).
[39]T. R. Roberts and S. G. Sydoriack, Phys. Rev. 102, 304 (1956).
[40]J. R. Clement and E. H. Quinell, Rev. Sci. Instr. 23, 213 (1952).
[41]See, e.g., E. F. Westrum, Jr., G. T. Furukawa, and J. P. McCullough, in *Experimental Thermodynamics*, edited by J. P. McCullough and D. W. Scott (Plenum, N. Y., 1968), Vol. I, Chap. 5, p. 187.
[42]G. Ahlers, Rev. Sci. Instr. 37, 477 (1966).
[43]R. W. Hill and O. V. Lounasmaa, Phil. Mag. 2, 143 (1957).
[44]D. T. Grimstrud and J. H. Werntz, Jr., Phys. Rev. 157, 181 (1967).
[45]A. Von Itterbeck and W. de Laet, Physica 24, 59 (1958).
[46]G. Ahlers, J. Phys. Chem. Solids 28, 525 (1967).
[47]M. E. Fisher, J. Math. Phys. 5, 944 (1964).
[48]M. E. Fisher, Repts. Progr. Phys. 30, 615 (1967).
[49]L. Onsager, Phys. Rev. 65, 117 (1944).
[50]See, for example, A. Ralson, *A First Course in Numerical Analysis* (McGraw-Hill, New York, 1965), Chap. 6.
[51]R. B. Griffiths (private communication).
[52]H. C. Kramers, J. D. Wasscher, and C. J. Gorter, Physica 18, 329 (1952).